Observability of the magnetic band structure of lateral superlattices

P. Rotter, M. Suhrke, and U. Rössler
Institut für Theoretische Physik, Universität Regensburg, D-93040 Regensburg, Germany
(Received 16 January 1996; revised manuscript received 1 March 1996)

We present a quantum mechanical calculation of the resistivity of a strongly modulated two-dimensional electron gas in a perpendicular magnetic field. For lattice constants of the order of the Fermi wavelength the classical picture of commensurate orbits breaks down and the magnetic band structure gains considerable influence. As a characteristic feature the longitudinal magneto-resistivity shows oscillations with a leading period of one flux quantum per unit cell which have their origin in the magnetic band structure. We find that they do only weakly depend on temperature and electron density and discuss the resulting necessary conditions for experimental observation. [S0163-1829(96)03228-6]

Magnetotransport experiments on antidot superlattices[1–4] have led to a variety of theoretical concepts[5–9] to uncover the underlying transport mechanisms. The first experimental results on GaAs/$Al_xGa_{1-x}As$ heterostructures were obtained for antidot lattice constants a far above the Fermi wavelength λ_F of the electrons. The observed commensurability peaks in the longitudinal component ρ_{xx} of the resistivity tensor gave rise to the classical picture of pinned orbits around a geometry dependent number of antidots.[5] Additional oscillations in ρ_{xx}, superimposed onto the commensurability peak for one antidot, have been observed at low temperatures.[2] Within a semiclassical theory for the conductivity these oscillations with a geometry dependent period of *approximately* one flux quantum per unit cell of the superlattice have been ascribed to the shortest periodic orbits trapped between some antidots or encircling a single antidot.[8,9] A quantum mechanical transport theory, which fully takes into account the magnetic band structure,[10,12,13] has been shown to reproduce all the mentioned findings in the classical regime ($a \gg \lambda_F$).[6,9] In the quantum regime, when a approaches λ_F (or becomes even smaller), one expects new characteristic features which are still to be detected in future transport experiments. The first direct resolution of a magnetic band structure might have been seen in a recent magneto-transport experiment with small lattice constants via a splitting of the usual Shubnikov–de Haas peaks into subpeaks for certain values of the magnetic flux.[4]

In this paper we present a calculation of the resistivity for a strongly modulated two-dimensional electron gas ($E_F \gtrsim V_0$) in the quantum regime. In addition to classical and semiclassical effects with strong temperature dependences we find quantum oscillations which are not affected by a change in temperature. As their origin is the dependence of the band structure on the magnetic field,[10–13] the leading period is *exactly* one flux quantum per unit cell. They differ from oscillations with period $1/B$ in the resistivity of a weakly modulated two-dimensional electron gas ($E_F \gg V_0$) (Ref. 14) caused by a similar mechanism. The reason for investigating a strongly modulated system and not the antidot regime ($E_F < V_0$) is twofold: The quantum oscillations are better observable in the resistivity and an experimental realization seems to be easier to achieve.

Since our model was described in detail elsewhere,[6,10] we mention only the essential ingredients: Using an effective mass single-particle Hamiltonian for a two-dimensional electron in a periodic potential and a perpendicular magnetic field, we calculate for rational values of flux quanta per unit cell the magnetic band structure $E_n(\vec{\Theta})$ (depending on the magnetic wave vector $\vec{\Theta}$ and the miniband index n) as well as the corresponding eigenstates. Impurity scattering is incorporated in self-consistent Born approximation (SCBA) which results in a broadening of states due to the finite lifetime. The static conductivity tensor is calculated with the Kubo formula. Finally, tensor inversion gives the components of the resistivity tensor which can be compared to a typical four-terminal measurement. The influence of temperature is taken into account in the calculations only via the Fermi function, i.e., temperature dependent scattering mechanisms are neglected in the temperature range considered ($T < 15$ K). This is justified because phase breaking by electron-electron and electron-phonon scattering occurs on a length scale larger than the thermal length $L_T = \hbar v_F / kT$ introduced by energy averaging (cf., e.g., Refs. 15 and 16). The periodic potential is modeled by

$$V(x,y) = V_0(\cos[(\pi/a)x]\cos[(\pi/a)y])^{2\beta}. \qquad (1)$$

The parameters $a = 100$ nm for the lattice constant, $V_0 = 5$ meV for the amplitude, and $\beta = 1$ for the steepness used throughout this paper are representative of a strongly modulated system at typical densities $n_s \simeq (1-3) \times 10^{15}$ m^{-2} corresponding to $E_F \simeq 4-12$ meV or $\lambda_F \simeq 75-40$ nm.

An overview of the calculated band structure is given in Fig. 1. The projection of the bands onto the energy axis is plotted versus the magnetic field between one and 4.5 magnetic flux quanta n_ϕ per unit cell of the superlattice. Throughout the paper we used all the integer multiples of 1, $\frac{1}{2}$, $\frac{1}{3}$, $\frac{1}{4}$, and $\frac{1}{8}$ within the denoted flux range. Especially for small flux values a strong dispersion can be found for integer values of n_ϕ with strongly overlapping bands identified in the projection as long unbroken lines. For noninteger values the bands split into minibands with additional gaps in between,[10–13] i.e., the dispersion of the minibands is significantly lower for the noninteger flux values than for the integer ones. With increasing magnetic field the bands cluster

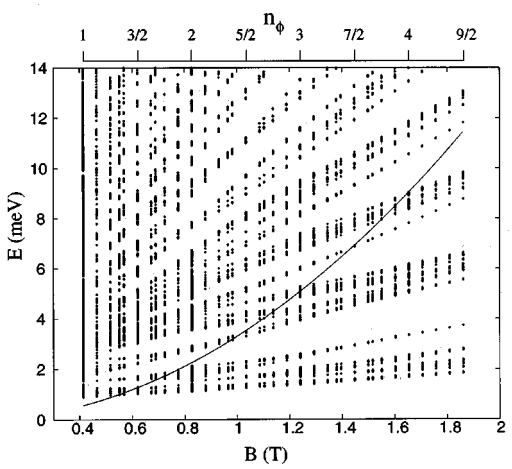

FIG. 1. Projection of the band structure onto the energy axis versus the magnetic field. n_ϕ indicates the rational number of elementary flux quanta per unit cell. The full curve shows the condition $2R_c=a$ to indicate the transition from periodic potential to magnetic field dominated band structure.

more and more towards the unperturbed Landau levels of the unmodulated two-dimensional electron gas. Together with the overall decrease of the dispersion this can be ascribed to the reduced influence of the periodic potential modulation. This occurs roughly if the cyclotron diameter approaches the lattice constant $2R_c=a$ (cf. full line in Fig. 1), usually known as the commensurability condition for the classical peak due to a pinned orbit around one antidot.

In order to visualize the connection between band structure, thermodynamic density of states $D(E_F)$, and longitudinal conductivity $\sigma_{xx}(E_F)$, these quantities are compared in Fig. 2 for three flux values (a) $n_\phi=1$, (b) $n_\phi=\frac{9}{8}$, and (c) $n_\phi=\frac{3}{2}$. The assumed mobility is $\mu=50\ \mathrm{m}^2/\mathrm{V\,s}$. In the first panel the energy bands are given for the lines Γ-A and Γ-M of the magnetic Brillouin zone, corresponding to the (10) and (11) directions, respectively; the positions of the unperturbed Landau levels are indicated in the middle. The strong dependence of the miniband structure on n_ϕ (for similar magnetic fields but different denominators of the rational flux values) does not influence the thermodynamic density of states (middle panel: $T=4$ K, full line; $T=15$ K, dotted line). Its effect on the longitudinal conductivity, however, is dramatic (right panel). In these figures we show $\sigma_{xx}(E_F)$ at 4 K (solid line) and 15 K (dotted line) together with the miniband conductivity at 4 K (dashed line). The latter results from the velocity matrix elements between states from the same minibands (which are large if the miniband has pronounced dispersion), in contrast to the scattering conductivity with matrix elements between states from different minibands.[6] This distinction is similar to the one introduced in Ref. 14 for the weak modulation case where, however, Landau levels are still well separated and scattering contributions are those with matrix elements nondiagonal in the Landau quantum number.

For $n_\phi=1$ the magnetoconductivity σ_{xx} is dominated by the miniband contribution due to the strong dispersion. A glance at the band structure makes clear that the most dispersive bands correspond to the maxima in σ_{xx}. The conductivity is strongly suppressed for $n_\phi=\frac{9}{8}$ (note the scales),

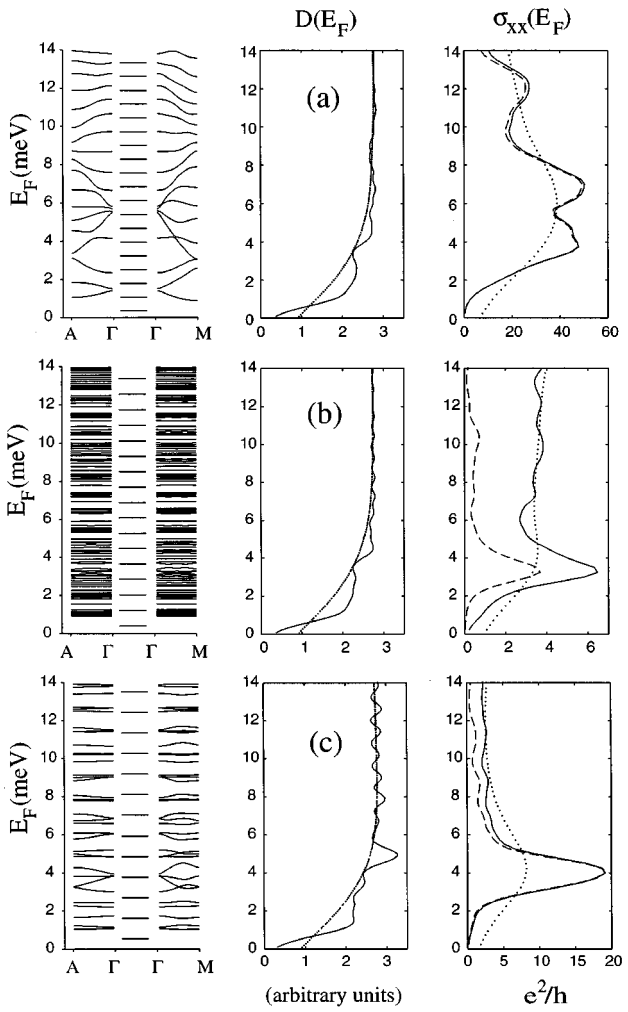

FIG. 2. Band structure, thermodynamic density of states, and longitudinal conductivity ($\mu=50\ \mathrm{m}^2/\mathrm{V\,s}$) for three values of the magnetic flux, (a) $n_\phi=1$, (b) $n_\phi=\frac{9}{8}$, and (c) $n_\phi=\frac{3}{2}$. The full lines show the values for $T=4$ K and the dotted ones those for $T=15$ K. The dashed line in the conductivity plot gives the band contribution for $T=4$ K.

with only a small miniband contribution, i.e., σ_{xx} is dominated by scattering between almost dispersionless minibands. For $n_\phi=\frac{3}{2}$ it recovers to some extent with again a significant contribution due to the miniband dispersion. The comparison of the $T=4$ and 15 K curves clearly shows that only the fine structure is smeared out by temperature broadening, but the order of magnitude of the conductivity is not changed. Therefore in the regime of strong modulation neither the temperature nor the position of the Fermi energy (fixed by the density of the electrons) have considerable influence on the suppression of the band conductivity, when the flux changes from integer to rational values. In the magnetic field dependence of σ_{xx} and, after tensor inversion, of ρ_{xx} and ρ_{xy} this leads to oscillations, which are (almost) independent of temperature and electron density and have their quantum mechanical origin in the magnetic field dependent miniband structure.

In Fig. 3 we show the longitudinal resistivity ρ_{xx} for $\mu=50\ \mathrm{m}^2/\mathrm{V\,s}$ in dependence on the magnetic field for different electron densities $n_s=(1.6\text{–}3.0)\times10^{15}\ \mathrm{m}^{-2}$ (increasing from bottom to top with $\Delta n_s=0.1\times10^{15}\ \mathrm{m}^{-2}$, offset for

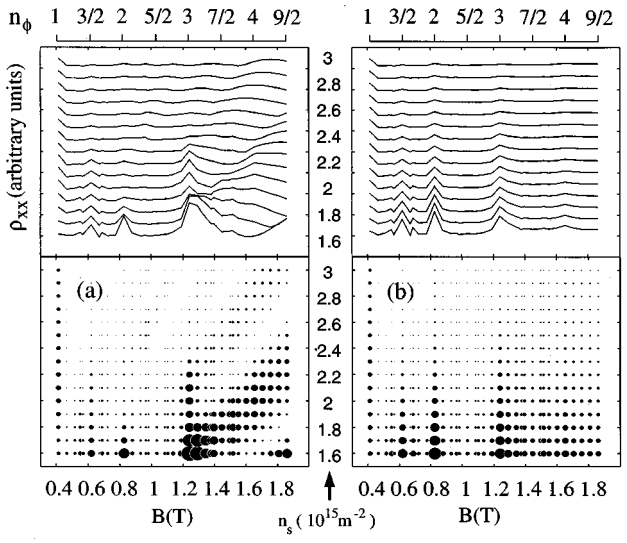

FIG. 3. Longitudinal resistivity ρ_{xx} versus the magnetic field for several electron densities ranging from $n_s = 1.6\times10^{15}$ m^{-2} at the bottom to $n_s = 3.0\times10^{15}$ m^{-2} at the top with $\Delta n_s = 0.1\times10^{15}$ m^{-2} and temperatures (a) $T = 4$ K and (b) $T = 15$ K and $\mu = 50$ m^2/V s. The curves are displaced along the vertical axis by a fixed value. In the lower part the size of the dots scales with the magnitude of ρ_{xx} to visualize the peak positions.

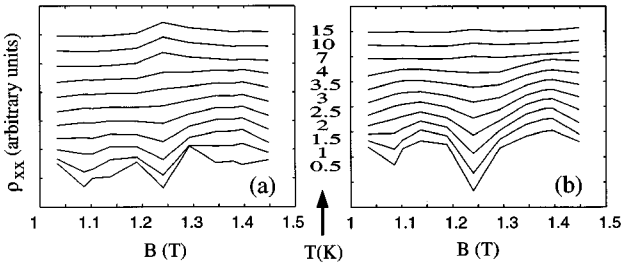

FIG. 4. Temperature dependence of the longitudinal resistivity ρ_{xx} around the $n_\phi = 3$ peak for an electron density of $n_s = 2.4\times10^{15}$ m^{-2} and for two different mobilities (a) $\mu = 50$ m^2/V s and (b) $\mu = 5$ m^2/V s. The temperature ranges from $T = 0.5$ K at the bottom to $T = 15$ K at the top. Again the curves are displaced along the vertical axis by a fixed amount.

clarity) and two temperatures, (a) $T = 4$ K and (b) $T = 15$ K. In the lower part of the figure the dot size indicates the magnitude of ρ_{xx} to make the position of the maxima and minima easier to comprehend. The range of electron densities corresponds to Fermi energies between 7 and 12 meV and allows us to tune from the strong ($E_F \geqslant V_0$) towards the weak modulation case ($E_F \gg V_0$). Two types of structures can be distinguished: (i) The most pronounced ones for $n_\phi = 1, \frac{3}{2}, 2$, and 3 do not change their position with n_s or T and decrease in amplitude with increasing n_s and (ii) Shubnikov–de Haas type structures (mainly above $B = 1.2$ T), which shift to higher magnetic fields with increasing n_s and disappear at higher temperatures. For the lowest curve the Fermi energy of 7 meV at $B \approx 1.2$ T coincides with the minibands which evolve into the third Landau level (see Fig. 1). With increasing electron density this coincidence is shifted to higher magnetic field as does the broad structure that evolves from the dominant peak around $B = 1.2$ T. At higher densities a similar but weaker structure shows up in connection with the fourth Landau level. These structures, which disappear at higher temperature [see Fig. 3(b)], can be described also by semiclassical concepts.[8] In contrast, the features which do not shift with changing electron density and persist even at higher temperature derive from magnetic field dependent miniband structure. They will be called quantum peaks. Note that for 4 K [Fig. 3(a)] these peaks react differently on changing n_s depending on the position of E_F relative to the gaps in the miniband structure. As for higher temperatures the gaps lose their relevance, all quantum peaks decrease almost simultaneously with increasing n_s [see Fig. 3(b)].

In our calculations for the regime of strong modulation the Hall conductivity σ_{xy} (not displayed here) is much larger than σ_{xx} and has no structures correlated with those of σ_{xx} [in contrast to the antidot regime $E_F < V_0$ (Ref. 9)]. Therefore we have $\rho_{xx} \propto \sigma_{xx}$ and peaks in σ_{xx} due to large miniband conductivity for rational n_ϕ with small denominators lead to pronounced maxima also in ρ_{xx} at $n_\phi = 1, \frac{3}{2}, 2$, and 3. Smaller structures in ρ_{xx} can be detected for $n_\phi = 4$ (at 15 K).

Figure 4 shows the distinct dependence on the temperature and on the mobility of these quantum peaks in comparison with the semiclassical oscillations for magnetic fields around $B = 1.25$ T (corresponding to $n_\phi = 3$). Here ρ_{xx} is displayed for temperatures between 0.5 and 15 K (from bottom to top) for the two mobilities (a) $\mu = 50$ m^2/V s and (b) $\mu = 5$ m^2/V s and an electron density $n_s = 2.4\times10^{15}$ m^{-2}. For the higher mobility [Fig. 4(a)] the rich structure at low temperature can hardly be interpreted because of the coexistence of semiclassical and quantum peaks. However, with increasing temperature only the quantum peak for $n_\phi = 3$ survives and stabilizes for $T > 5$ K, while all other structures vanish. Lowering the mobility by a factor of 10 [Fig. 4(b)] essentially destroys the quantum peak. This can be explained by the fact that now the scattering contribution dominates the longitudinal conductivity and the reduction of the band conductivity for noninteger fluxes plays only a minor role. Only the semiclassical features survive this increase of scattering strength. In the Hall conductivity σ_{xy} (not displayed here) small dips start to develop for $n_\phi = 2,3,4$ (compare Ref. 9). However, they are far too small to yield a significant contribution in the resistivities.

Thus we are able to predict the conditions for an experimental observation of quantum oscillations that derive from the miniband structure. Generally, a high band conductivity is a necessary condition for this effect. The most important requirements are small lattice constants, whereas an extraordinary high mobility has not to be accomplished. For the usual experimental mobilities of $\mu = 50$ m^2/V s calculations for larger lattice constants show that periods of about 100 nm have to be achieved. For a comparatively soft potential the peaks are most clearly detectable in the strong modulation regime, as is shown by calculations for the antidot case not displayed here. However, the former might be easier to realize at small lattice constants. A useful hint for the identification of the quantum peaks is provided by the independence of the maxima in ρ_{xx} on the electron density. These peaks are destroyed with increasing temperature if the phase coherence length becomes smaller than the lattice period. This occurs, however, at a higher temperature than that necessary for the destruction of energy dependent interference effects such as,

e.g., Shubnikov–de Haas oscillations governed by L_T. Consequently, there should be a window for an exclusive observation of the quantum peaks for not too low temperature. This gives rise to the hope that these quantum mechanical features can be seen in the near future. One possible reason for a significant suppression of the quantum oscillations, however, not considered in our calculations, is fluctuations of the lattice constant in experiments on macroscopic samples. Thus an important experimental prerequisite is either a macroscopic homogeneous sample or a finite small sample if boundary effects can be eliminated.

In conclusion we have demonstrated in this paper the effect of band structure on the transport properties of a strongly modulated two-dimensional electron gas in a perpendicular magnetic field. For high mobility samples structured by a superlattice with small lattice constants, we have calculated the resistivities as a function of magnetic field, electron density, and temperature. We have found characteristic oscillations periodic in the magnetic flux, especially for small magnetic fields. They can be distinguished from classical and semiclassical oscillations by their stability against changes in electron density. These quantum peaks, which at lower temperatures ($T \lesssim 4$ K) can hardly be distinguished from the other coexisting structures, are the only ones that survive for higher temperatures ($T > 10$ K) until they disappear due to the decreasing phase coherence length. Thus we have established necessary conditions for an experimental observation.

We thank the Deutsche Forschungsgemeinschaft for financial support within Sonderforschungsbereich 348. Most of the calculations have been done on the Cray Y-MP supercomputers at the Leibniz Rechenzentrum Munich and at the HLRZ Jülich. Stimulating discussions with K. Ensslin, T. Schlösser, and D. Weiss are gratefully acknowledged.

[1] D. Weiss *et al.*, Phys. Rev. Lett. **66**, 2790 (1991); A. Lorke *et al.*, Superlatt. Microstruct. **9**, 103 (1991); R. Schuster *et al.*, *ibid.* **12**, 93 (1992).
[2] D. Weiss *et al.*, Phys. Rev. Lett. **70**, 4118 (1993).
[3] R. Schuster *et al.*, Phys. Rev. B **49**, 8510 (1994).
[4] T. Schlösser *et al.*, Europhys. Lett. **33**, 683 (1996).
[5] R. Fleischmann *et al.*, Phys. Rev. Lett. **68**, 1367 (1992).
[6] H. Silberbauer and U. Rössler, Phys. Rev. B **50**, 11911 (1994).
[7] R. B. S. Oakeshott and A. MacKinnon, J. Phys. Condens. Matter **6**, 1519 (1994).
[8] K. Richter, Europhys. Lett. **29**, 7 (1995); G. Hackenbroich and F. von Oppen, *ibid.* **29**, 151 (1995).
[9] S. Ishizaka *et al.*, Phys. Rev. B **51**, 9881 (1995).
[10] H. Silberbauer, J. Phys. Condens. Matter **4**, 7355 (1992).
[11] R. Peierls, Z. Phys. **80**, 763 (1933); H. J. Fischbeck, Phys. Status Solidi **38**, 11 (1970); J. Zak, in *Solid State Physics: Advances in Research and Applications*, edited by H. Ehrenreich *et al.* (Academic Press, New York, 1972), Vol. 27, p. 1.
[12] P. G. Harper, Proc. R. Soc. London Ser. A **68**, 874 (1955); M. Y. Azbel, Zh. Éksp. Teor. Fiz. **46**, 929 (1966) [Sov. Phys. JETP **19**, 634 (1964)].
[13] D. R. Hofstadter, Phys. Rev. B **14**, 2239 (1976).
[14] D. Pfannkuche and R. R. Gerhardts, Phys. Rev. B **46**, 12 606 (1992).
[15] A. Yacoby *et al.*, Phys. Rev. Lett. **66**, 1938 (1991); **73**, 3149 (1994).
[16] C. Kurdak *et al.*, Phys. Rev. B **46**, 6846 (1992).